J1.2 INDIRECT IMPACT OF ATMOSPHERIC AEROSOLS IN IDEALIZED SIMULATIONS OF CONVECTIVE-RADIATIVE QUASI-EQUILIBRIUM

Wojciech W. Grabowski*
NCAR†, Boulder, Colorado

1. INTRODUCTION.

Indirect impact of atmospheric aerosols concerns the impact on the formation of cloud and precipitation particles, and it is one of the most uncertain aspects of the anthropogenic climate change. The type and concentration of cloud condensation nuclei (CCN) affect the concentration of nucleated cloud droplets. For the same cloud water content, higher concentration of cloud droplets implies smaller droplet size and thus higher albedo. This is the first indirect aerosol effect, also known as the Twomey effect (Twomey 1974, 1977). Moreover, smaller cloud droplets (for the same cloud water content) result in a slower development of drizzle and rain via the collisions/coalescence (e.g., Warner 1968). This can potentially affect the abundance, extent, and lifetime (hence the time-averaged albedo) of some types of clouds, such as stratocumulus or shallow convective clouds (e.g., Albrecht 1989, Pincus and Baker 1994). This is the second indirect aerosol effect. Indirect effects are typically investigated either using general circulation models, which have to relay on cloud parameterizations and thus provide questionable predictions, or in relatively short cloud-resolving model (CRM) simulations whose relevance to the climate problem is not always clear. Herein we present results of idealized cloud-resolving simulations of convective-radiative quasi-equilibrium mimicking the mean climate of Earth and investigate the indirect aerosol effects in this relatively simple system. The extended version of this discussion is presented in Grabowski (2006).

The modeling setup is the convective-radiative quasi-equilibrium with fixed surface characteristics mimicking the mean conditions on Earth (the surface temperature of 15 deg C, surface albedo of 0.15, and surface relative humidity of 85%) and prescribed mean solar input of 342 W m^{-2}, see Fig. 7 in Kiehl and Trenberth (1997; hereafter KT97). The simulations concern only the impact on warm rain microphysics, and impacts on ice processes are not considered. The motivation to focus on warm rain processes are the following. First, warm-rain processes are relatively well understood (especially when compared to ice processes), and the role of cloud microphysics can be simulated with better confidence. Second, anthropogenic changes of atmospheric aerosols are dominated by increased concentrations of soluble aerosols acting as CCN. Finally, warm shallow clouds are abundant both in the Earth atmosphere and in the idealized simulations discussed here, and they have more significant impact on the radiative transfer than deep clouds, at least in the tropics (cf. Kiehl 1994).

* *Corresponding author address*: Dr. W. W. Grabowski, NCAR, PO Box 3000, Boulder, CO 80307; e-mail: grabow@ncar.ucar.edu.

† NCAR is sponsored by the National Science Foundation.

2. THE MODEL AND MODELING SETUP.

The dynamic model is a stand-alone version of the superparameterization model used in simulations described in Grabowski and Smolarkiewicz (1999) and Grabowski (2001; 2002; 2003; 2004), with some modifications. It assumes 2D geometry with periodic lateral boundary conditions, applying a relatively small horizontal domain covering 200 km with a horizontal grid length of 2 km. In the vertical, the model applies a stretched grid with 61 levels covering the troposphere and lower stratosphere (up to 24 km). The stretched grid applies about a dozen levels in the lowest 2 km which is essential to represent shallow convection and boundary layer processes. Tests using observationally-based model intercomparison cases for LES and CRM models (e.g., BOMEX case, Siebesma et al. 2003; ARM shallow convection case, Brown et al. 2002; LBA case, Grabowski et al. 2006) demonstrate that this model configuration, together with a nonlocal boundary layer scheme (e.g., Troen and Mahrt 1986) is capable in representing boundary layer processes and shallow convection (e.g., the vertical structure of mean fields and fluxes, diurnal cycle of the boundary layer depth and cloudiness, etc). The model solves nonhydrostatic anelastic equations using the nonoscillatory forward-in-time integration scheme (Smolarkiewicz and Margolin 1997), and it applies bulk cloud microphysics with a simple representation of warm-rain and ice processes (Grabowski 1998).

The radiation transfer model comes from the NCAR's Community Climate System Model (Kiehl et al. 1994). A diurnal cycle of solar radiation is not considered, the solar constant is reduced to 342 W m^{-2} (i.e., the nominal solar constant averaged over the entire planet, cf. Fig. 7 in KT97), and a zero zenith angle is assumed. The radiation model is applied in the independent column approximation mode, i.e., radiation transfer is calculated in all cloud model columns independently from each other. Radiation calculations are performed every model time step, i.e., every 20 seconds.

The simulations start from the midlatitude summertime sounding which has a near-surface temperature of about 20 deg C. Since the surface temperature is assumed at 15 deg C, the mean temperature and moisture profiles experience significant adjustments during the first few weeks of the simulations. The mean horizontal wind at all levels is assumed 4 m/s and is maintained by relaxing the mean wind profile toward the initial one using a one hour time scale. The simulations are run for 120 days with quasi-equilibrium reached after about 60 days. Days 91-120 are used in the analysis.

The simulations described here investigate the sensitivity of convective-radiative quasi-equilibrium to changes of the assumed number concentration of cloud droplets and to changes in the formulation of the effective radius (assumed to be equal to the mean volume radius) of cloud droplets in diluted clouds. Two sets of model simulations are performed with different concentrations of cloud droplets, either 100 cm^{-3} (referred to as PRISTINE cases) or 1000 cm^{-3} (referred to as POLLUTED cases). The difference in droplet concentration has two effects, consistent with the two indirect aerosol effects.

The first indirect aerosol effect is represented in the model by various formulations of the local value of the effective radius. For ice, the effective radius depends on the combined ice and snow water content based on measurements in tropical anvils reported by McFarquhar and Heymsfield (1997), see eq. (2) in Grabowski (2000). The effective radius of cloud droplets is prescribed by referring to various "mixing scenarios" because the main issue is in the formulation of the effective radius in diluted cloud volumes. Similarly to Chosson et al. (2004), we consider the homogeneous and extremely inhomogeneous mixing scenarios, but we also consider an intermediate scenario based on simulations discussed in Andrejczuk et al. (2004, 2006). These formulations are briefly discussed below.

1. *The homogeneous mixing scenario.* Assuming that the cloud droplet concentration is known (i.e., 100 cm^{-3} in PRISTINE or 1,000 cm^{-3} in POLLUTED), the mean volume radius of cloud droplets is calculated from the local cloud water mixing ratio and the assumed cloud droplet concentration. This formulation implies that, for the same cloud water content, the ratio between effective radii for PRISTINE and POLLUTED cases is $10^{(1/3)}$, which is about 2.2. We refer to this formulation as corresponding to the homogeneous mixing scenario, because any dilution of a cloud due to entrainment is always assumed to reduce droplet size but not the concentration, i.e., all droplets are assumed to be exposed to the same environmental conditions (hence term homogeneous mixing). In reality, homogeneous mixing involves also a change of droplet concentration, with the concentration in a diluted parcel smaller by a factor depending on the proportion of the cloudy air in the mixture. This effect in neglected in the current study.

2. *The extremely inhomogeneous mixing scenario.* In contrast to the homogeneous mixing, one can assume that any cloud dilution results in a decrease of droplet concentration but not the size of cloud droplets. In other words, cloud dilution results in a complete evaporation of some droplets, whereas the rest do not change their sizes at all. This corresponds to the extremely inhomogeneous mixing scenario (Baker and Latham 1979; Baker et al. 1980). In this case, the mean volume radius of cloud droplets is a function of height only, regardless of the local value of the cloud water mixing ratio. The mean volume radius is calculated (separately for PRISTINE and POLLUTED cases) using a simple raising parcel model (which provides adiabatic liquid water content at any model level) and applying the assumed cloud droplet concentration. At any given height, the effective radius for the PRISTINE case is again about 2.2 larger than for the POLLUTED case.

3. *The intermediate mixing scenario.* This case represents a combination of the two mixing scenarios above, i.e., both the size of cloud droplets and their concentration is assumed to change due to cloud dilution. This scenario is suggested by recent direct numerical simulations of microscale homogenization described in Andrejczuk et al. (2004, 2006). In a particular implementation herein, it is assumed that in the diluted cloudy volumes, the number of cloud droplets and their volume (i.e., the mean volume radius cubed) change in the same proportion. This corresponds to the limiting case of the turbulent mixing with low turbulent kinetic energy in Andrejczuk et al., i.e., along a diagonal on the mixing diagram that represents the changes in the mean volume radius as a function of the changes of the number of cloud droplets; see Grabowski (2006) for more details.

The second indirect aerosol effect is represented in the model through the Berry's formulation of the conversion from cloud water to rain (Berry 1968). In this formulation, the conversion term depends on the assumed number concentration of cloud droplets and the width of the cloud droplet spectrum. The latter is assumed larger in the PRISTINE case, with nondimensional cloud droplet spectral dispersion (the ratio between the standard deviation and the mean) equal to 0.32 and 0.19 in PRISTINE and POLLUTED simulations, respectively. The collection efficiency for rain collecting cloud water is assumed the same in PRISTINE and POLLUTED cases (0.8), whereas in reality it weakly depends on the typical size of cloud droplets as well.

In summary, three simulations are performed for the PRISTINE conditions and three for the POLLUTED. In each simulation, the assumed cloud droplet concentration impacts the formulation of the effective radius in radiative transfer and affects autoconversion of cloud water to drizzle and rain as discussed above. Except for these differences, the simulations are otherwise identical. In particular, all simulations consider the same conditions in clear air, whereas in reality one might expect some differences due to higher concentration of absorb-

ing aerosols outside clouds in the POLLUTED case. Such direct aerosol radiative effects, however, are not considered here and the differences between PRISTINE and POLLUTED cases are due to the first and the second indirect effect only. Model results are compared with the mean components of the Earth energy budget as discussed in KT97.

3. RESULTS.

The quasi-equilibrium temperature and moisture profiles in all simulations differ little. For instance, for the simulations PRISTINE and POLLUTED with homogeneous mixing scenario, the maximum temperature difference is about 0.2 K and it occurs just above the boundary layer. The maximum relative humidity difference (about 4%) occurs in the lower troposphere. Figure 1 illustrates quasi-equilibrium statistics of simulated clouds. It shows profiles of cloud fraction (defined at any level as the fraction of model gridboxes with cloud condensate larger than 0.01 g kg^{-1}), and horizontally-averaged cloud condensate and precipitation mixing ratios, for simulations PRISTINE and POLLUTED with homogeneous mixing scenario. The figure documents the importance of the lower-tropospheric cloudiness and shows that the mean cloud profiles are similar in PRISTINE and POLLUTED simulations. The lower cloud fraction and lower cloud condensate between 1 and 5 kilometers in the simulation PRISTINE is consistent with more rapid formation of precipitation in warm clouds in this simulation. Although the difference between the two profiles is comparable to the standard deviations of their temporal evolution, a Student's t-test shows that the difference is significant at 0.001 probability level. The slightly smaller mean precipitation rate in POLLUTED simulation (right panel in Fig. 1) seems inconsistent with the setups of model simulations, but it is not statistically significant.

The key results of this study are summarized in Table 1, which provides water and energy fluxes as simulated in cases PRISTINE and POLLUTED and compares them to the diagnosed fluxes presented in KT97. In general, the overall agreement between model simulations and KT97 planetary-mean fluxes is surprising, considering the simplifications of the numerical model and the modeling setup, where the entire atmospheric dynamics in the Earth climate is reduced to the convective-radiative quasi-equilibrium over a small area. The table shows that the indirect impact of atmospheric aerosols concerns mostly solar radiation, with the most significant differences between the simulations being the impact on the net TOA solar flux (and thus the TOA albedo) and the amount of solar energy reaching the surface. The impact on the longwave fluxes is insignificant, so is the impact on the hydrologic cycle: the surface precipitation rates and the partitioning of the total surface heat flux into the sensible and latent components are virtually the same in all simulations.

The most significant impact of the assumed cloud droplet concentration and the formulation of the effective radius occurs at the surface. In general, model results are consistent with the expectation that more numerous cloud droplets result in larger TOA albedo and smaller solar flux absorbed at the surface. The change of cloud droplet size can be obtained either by changing the assumed droplet concentration (from PRISTINE to POLLUTED) or by changing the formulation of mean droplet size in regions modified by entrainment (from extremely inhomogeneous, through intermediate, to homogeneous). The change from PRISTINE to POLLUTED conditions — for the same formulation of the effective radius — results in about 20 W m^{-2} decrease of the net surface energy budget. However, changing the formulation of the effective radius has a similar effect. For instance, the PRISTINE simulation with effective radius formulated according to the homogeneous mixing has the same

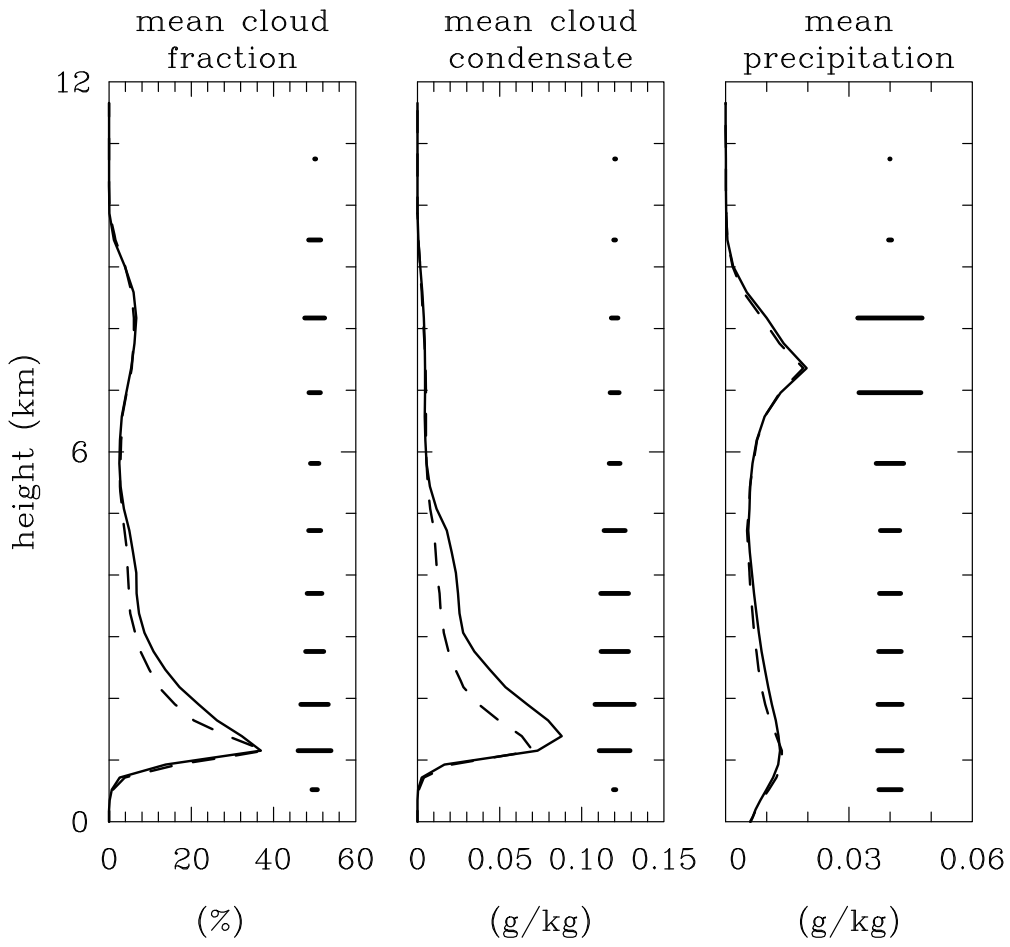

Figure 1: Quasi-equilibrium profiles (averages over days 91-120) of the cloud fraction, cloud condensate, and precipitation mixing ratios for simulations POLLUTED (solid line) and PRISTINE (dashed line) with homogeneous mixing scenario. The length of horizontal bars to the right of each profile represent the average standard deviation (i.e., the mean of the POLLUTED and PRISTINE) of the temporal evolution of the domain-mean. The bars are shown only at selected levels.

surface energy budget as the POLLUTED simulations and the extremely inhomogeneous mixing scenario. It follows that the formulation of the spatial variability of the effective radius impacts the surface energy budget at the same degree as the Twomey effect itself!

Table 1: Energy fluxes averaged over 30-day period (days 91-120) for various simulations assuming PRISTINE and POLLUTED cloud conditions. Columns marked "h", "ei", and "r-N" show results from simulations where, respectively, homogeneous, extremely inhomogeneous, and intermediate mixing scenarios were assumed to prescribe the effective radius of cloud droplets. Values in brackets show standard deviations for the 30-day averaging period. Estimates of global mean energy budgets from Kiehl and Trenberth (1997) are shown in KT97 column.

	PRISTINE			**POLLUTED**			**KT97**
	100 per cc			1,000 per cc			
	h	r-N	ei	h	r-N	ei	
net TOA shortwave flux (W m^{-2})	225 (12)	239 (8)	245 (6)	201 (10)	219 (10)	225 (9)	235
TOA albedo	0.34 (0.03)	0.30 (0.03)	0.28 (0.03)	0.41 (0.03)	0.36 (0.03)	0.34 (0.03)	0.31
OLR (W m^{-2})	242 (3)	243 (4)	243 (3)	240 (3)	242 (4)	242 (3)	235
radiative cooling of troposphere (W m^{-2})	-101 (4)	-100 (5)	-100 (5)	-101 (4)	-99 (4)	-99 (4)	-102
solar energy absorbed at surface (W m^{-2})	163 (11)	178 (10)	184 (8)	141 (12)	159 (12)	164 (10)	168
surface net longwave flux (W m^{-2})	73 (5)	73 (7)	73 (6)	70 (5)	73 (6)	73 (5)	66
surface sensible heat flux (W m^{-2})	20 (2)	19 (2)	20 (1)	19 (1)	19 (2)	18 (2)	24
surface latent heat flux (W m^{-2})	73 (2)	73 (2)	73 (2)	75 (2)	74 (2)	74 (2)	78
surface precipitation (W m^{-2})	69 (33)	69 (33)	70 (29)	72 (28)	71 (30)	70 (32)	78
surface energy budget (W m^{-2})	**-2 (7)**	**12 (6)**	**17 (5)**	**-23 (9)**	**-7 (8)**	**-2 (7)**	**0**

To better understand the key results concerning the impact of clouds on the solar radiation, the analysis of statistical properties of the optical depth of clouds present in the simulations was performed. The optical depth of a cloud is the ratio between geometric thickness of the cloud and the mean free path of photons traversing it. For nonabsorbing clouds (i.e., scattering only), the optical depth is formally defined as (e.g., Stephens 1978):

$$\tau = 2\pi \int_0^H \left[\int n(r) r^2 dr \right] \, dz \qquad (1)$$

where $n(r)$ is the local spectral density of cloud particles (i.e., the number of particles in the unit volume and the unit size interval r), and the integration in the vertical covers cloud depth H. By introducing the effective radius r_e, (1) can be rewritten as:

$$\tau = \frac{3}{2}\frac{1}{\rho_w}\int_0^H \frac{\rho_a q}{r_e}\, dz \tag{2}$$

where $q = 4/3\ \pi\rho_w \int n(r) r^3 dr\ /\rho_a$ is the mixing ratio of cloud condensate, and ρ_a and ρ_w are the densities of air and water, respectively. If more than one type of cloud particles is locally present (e.g., water droplets and ice crystals), the ratio q/r_e needs to be replaced by a sum of q^i/r_e^i, where q^i and r_e^i are mixing ratios and effective radii of all types of cloud particles. It should be pointed out that both the mixing ratio and the effective radius are, in general, functions of height in (2). One can define, however, the mean ("effective") effective radius of a cloudy column $\overline{r}_e$ as the radius that gives the optical depth (2) given the condensed water path $CWP = \int_0^H \rho_a q\ dz$, i.e.,

$$\overline{r}_e = \frac{3}{2}\ \frac{CWP}{\rho_w \tau}\ . \tag{3}$$

The critical point is that the changes in the $\overline{r}_e$ represent the first indirect effect, whereas the second effect is captured in changes of CWP. It follows that the changes of τ between various simulations can be separated into the impact on $\overline{r}_e$ and on CWP. To distinguish effects on water and ice clouds, τ, $\overline{r}_e$, and CWP can be separately calculated for liquid and solid cloud particles.

The mean values of of τ, CWP, and $\overline{r}_e$ separated into water and ice components are summarized in Table 2. The table shows that the differences in the mean water and ice cloud cover (defined as as a fraction of model columns with cloud optical depth larger than 1) are consistent with the second indirect effect. Slightly higher cloud fraction for ice clouds in the POLLUTED case is consistent with the expectation that more rapid formation of precipitation through the warm rain processes in PRISTINE simulations leads to less condensate inside upper-tropospheric ice clouds. Despite large temporal variability (i.e., the large standard deviations), some of the differences are statistically significant according to the Student's t-test. The mean optical depth for water clouds varies significantly between PRISTINE and POLLUTED with different mixing scenarios (roughly by a factor of 4 between PRISTINE with extremely inhomogeneous mixing and POLLUTED with homogeneous mixing). For both PRISTINE and POLLUTED clouds, the mean optical depth changes by more than 50% between homogeneous and extremely inhomogeneous mixing scenarios. This is significantly larger than the 35% change simulated by Chosson et al. (2004) for the case of stratocumulus. The differences between mean optical depth of ice clouds are insignificant. The results for LWP for PRISTINE and POLLUTED clouds differ significantly, with mean values for POLLUTED clouds roughly 50% larger than PRISTINE regardless of the mixing scenario. The difference is statistically significant at 0.001 probability level. This difference comes mostly from clouds with LWP larger than a few tenths of kg m^{-2}; the mean LWP for clouds with LWP smaller than 0.2 kg m^{-2} is only about 1% larger for POLLUTED than for PRISTINE clouds. The differences in the IWP are small and statistically insignificant. The large changes of the optical depth of water clouds are dominated by the changes of the mean effective radius $\overline{r}_e$, which also changes by a factor of about 4 between PRISTINE with extremely inhomogeneous mixing and POLLUTED with homogeneous mixing. Changes of $\overline{r}_e$ between various simulations are consistent with the assumptions concerning PRISTINE and POLLUTED simulations and with the assumed mixing scenarios.

In summary, Table 2 suggests that the difference between PRISTINE and POLLUTED simulations *for a given mixing scenario* is dominated by the first (Twomey) effect because the mean effective radius changes by a factor of about 2. The mean LWP (the second indirect effect) changes by a factor of about 1.4. Combined, these two factors explain the change of the mean cloud optical depth by a factor around 2.8 between PRISTINE and POLLUTED simulations for a given mixing scenario.

Table 2: Mean radiative properties of clouds averaged over 30-day period (days 91-120) for various simulations assuming PRISTINE and POLLUTED cloud conditions. Columns marked "h", "ei", and "r-N" are for simulations with, respectively, homogeneous, extremely inhomogeneous, and intermediate mixing scenarios. First two rows show percentage of columns with optical depth for water and ice clouds larger than one; third and fourth rows – the mean optical depth of water and ice clouds; fifth and sixth rows – the mean liquid and ice paths; seventh and eighth – the mean effective radii of water and ice clouds. All means are derived including only columns with optical depth larger than 1. Values in brackets show standard deviations for the 30-day averaging period.

	PRISTINE 100 per cc			**POLLUTED** 1,000 per cc		
	h	r-N	ei	h	r-N	ei
% of water	51	49	47	55	50	48
cloudy columns	(9)	(10)	(5)	(9)	(9)	(8)
% of ice	12	11	12	14	13	13
cloudy columns	(4)	(4)	(4)	(4)	(5)	(4)
water optical	32.1	24.7	20.5	89.0	64.8	57.4
depth (1)	(7)	(5)	(5)	(20)	(15)	(15)
ice optical	7.7	8.0	7.7	7.8	7.9	7.9
depth (1)	(4)	(4)	(4)	(4)	(5)	(5)
liquid water	0.23	0.24	0.23	0.33	0.33	0.33
path (kg m^{-2})	(0.05)	(0.05)	(0.06)	(0.09)	(0.09)	(0.10)
ice water	0.48	0.50	0.47	0.50	0.51	0.51
path (kg m^{-2})	(0.45)	(0.46)	(0.44)	(0.46)	(0.49)	(0.48)
water mean	8.3	12.3	14.9	4.1	6.1	7.4
r_e (μm)	(0.4)	(0.5)	(0.9)	(0.2)	(0.3)	(0.4)
ice mean	105	106	105	108	106	108
r_e (μm)	(20)	(23)	(22)	(19)	(20)	(20)

4. CONCLUSIONS

This paper discusses results from idealized simulations of convective-radiative quasi-equilibrium over a surface with fixed surface characteristics (surface albedo of 0.15, surface temperature of 15 deg C and relative humidity of 85%) and prescribed solar input (342 W m^{-2}), mimicking the mean conditions on Earth (Kiehl and Trenberth 1997). In the simulations, the cloud-resolving model, a stand-alone version of the 2D superparameterization model (e.g., Grabowski 2001; 2004) is coupled with the radiation transfer model from NCAR's Community Climate System Model (Kiehl et al. 1994). The focus is on

the impact of warm rain microphysics on water and energy fluxes across the atmosphere in convective-radiative quasi-equilibrium. Two limits of the concentration of cloud droplets are considered, either 100 cm^{-3}, reffered to as PRISTINE, or 1000 cm^{-3}, reffered to as POLLUTED. In addition, three formulations of the spatial variability of the effective radius are applied, corresponding to the homogeneous, intermediate, and extremely inhomogeneous mixing scenarios outside the adiabatic cloud volumes. The assumed concentration of cloud droplets, together with the mixing scenario, affects local values of the effective radius of cloud droplets applied in the radiation transfer model (the so-called first indirect aerosol effect, also known as the Twomey effect). Moreover, the assumed concentration of cloud droplets impacts the autoconversion of cloud water into drizzle and rain in the bulk microphysics scheme used in the cloud-resolving model. No impact on ice process is considered.

As on Earth, the cloud-resolving model cloudiness is dominated by shallow convection which justifies focusing on the impact of warm microphysics. In general, the convective-radiative quasi-equilibrium mimics the water and energy fluxes across the Earth's atmosphere to within less than 10 W m^{-2}. This implies that some of the feedbacks essential for the Earth climate system (such as the water vapor feedback, the cloud feedback, surface albedo and humidity feedbacks, etc.) can be efficiently studied using this relatively simple system. The indirect impact of warm microphysics is dominated by the first indirect effect, with less significant impact on the mean liquid water path (the second indirect effect), and virtually no impact on the hydrologic cycle. The latter highlights the difference between the impact of cloud microphysics on a single cloud from the impact on an ensemble of clouds. The key is that the fate of a single cloud, affected by the cloud microphysics, impacts subsequent clouds through the imprint the first cloud leaves within its environment. The conclusion about the smaller role of the second indirect effect has to be treated with caution as far as the Earth climate system is concerned because it is possible that this effect is more significant for different types of clouds than present in current simulations (e.g., stratocumulus). It is also feasible that the impact on the hydrologic cycle might turn out more significant once an interactive surface is included in the model physics. The latter aspect needs to be investigated in follow-up model simulations.

In convective-radiative quasi-equilibrium simulated by the model, the indirect effects impact the mean "planetary" albedo and thus the amount of solar energy reaching the surface, with all other components of atmospheric energy and water budgets virtually the same in all simulations. It follows that the indirect effects of aerosols occur mostly by impacting surface radiative fluxes, which is different from the direct effect where scattering and absorption of radiation by aerosols suspended in the atmosphere affects both the atmospheric and surface processes. The simulations suggest that the magnitude of the first indirect effect critically depends on the formulation of the spatial variability of the effective radius within clouds, especially in diluted volumes. For instance, the amount of solar energy reaching the surface is the same in the PRISTINE case assuming the homogeneous mixing scenario and in the POLLUTED case with the extremely inhomogeneous mixing. This result emphasizes the essential role of poorly understood microphysical transformations within highly diluted convective clouds and calls for focused research in this area. Aircraft observations, remote sensing, and numerical simulations are all capable of contributing to the progress.

Acknowledgements. This work was supported by the NOAA Grant NA05OAR4310107. National Center for Atmospheric Research is sponsored by the National Science Foundation.

REFERENCES

Albrecht, B. A., 1989: Aerosols, cloud microphysics, and fractional cloudiness. *Science*, **245**, 1227–1230.

Andrejczuk, M., W. W. Grabowski, S. P. Malinowski, and P. K. Smolarkiewicz, 2004: Numerical simulation of cloud-clear air interfacial mixing. *J. Atmos. Sci.*, **61**, 1726–1739.

Andrejczuk, M., W. W. Grabowski, S. P. Malinowski, and P. K. Smolarkiewicz, 2006: Numerical simulation of cloud-clear air interfacial mixing: Effects on cloud microphysics. *J. Atmos. Sci.* (in press).

Baker, M. B., and J. Latham, 1979: The evolution of droplet spectra and the rate of production of embryonic raindrops in small cumulus clouds. *J. Atmos. Sci.*, **36**, 1612–1615.

Baker, M. B., R. G. Corbin, and J. Latham, 1980: The influence of entrainment on the evolution of cloud droplet spectra: I. A model of inhomogeneous mixing. *Quart. J. Roy. Met. Soc.*, **106**, 581–598.

Berry, E. X., 1968: Modification of the warm rain process. *Proc. 1st Natl. Conf. on Weather Modification*, Albany, N.Y., Amer. Meteor. Soc., 81–85.

Brown, A. R., and Coauthors, 2002: Large-eddy simulation of the diurnal cycle of shallow convection over land. *Quart. J. Roy. Met. Soc.*, **128**, 1075–1094.

Chosson, F., J.-L. Brenguier, and M. Schröder, 2004: Radiative impact of mixing processes in boundary layer clouds. *Proceedings of the International Conference on Clouds and Precipitation*, Bologna, Italy, 371–374.

Grabowski, W. W., 1998: Toward cloud resolving modeling of large–scale tropical circulations: A simple cloud microphysics parameterization. *J. Atmos. Sci.*, **55**, 3283–3298.

Grabowski, W. W., 2000: Cloud microphysics and the tropical climate: cloud–resolving model perspective. *J. Climate*, **13**, 2306–2322.

Grabowski, W. W., 2001: Coupling cloud processes with the large-scale dynamics using the Cloud-Resolving Convection Parameterization (CRCP). *J. Atmos. Sci.*, **58**, 978–997.

Grabowski, W. W., 2003: MJO-like coherent structures: Sensitivity simulations using the Cloud-Resolving Convection Parameterization (CRCP). *J. Atmos. Sci.*, **60**, 847–864.

Grabowski, W. W., 2004: An improved framework for superparameterization. *J. Atmos. Sci.*, **61**, 1940–1952.

Grabowski, W. W., 2006: Indirect impact of atmospheric aerosols in idealized simulations of convective-radiative quasi-equilibrium. *J. Climate.* (in press).

Grabowski, W. W., and P. K. Smolarkiewicz, 1999: CRCP: A Cloud Resolving Convection Parameterization for modeling the tropical convecting atmosphere. *Physica D*, **133**, 171–178.

Grabowski, W. W., and Coauthors, 2006: Daytime convective development over land: a model intercomparison based on LBA observations. *Quart. J. Roy. Met. Soc.*, **132**, 317–344.

Kiehl, J. T., 1994: On the observed near cancellation between longwave and shortwave cloud forcing in tropical regions. *J. Climate*, **7**, 559–565.

Kiehl, J.T., J.J. Hack, and B.P. Briegleb, 1994: The simulated Earth radiation budget of the National Center for Atmospheric Research community climate model CCM2 and comparisons with the Earth Radiation Budget Experiment (ERBE). *J. Geophys. Res.*, **99**, 20,815–20,827.

Kiehl, J. T., and K. E. Trenberth, 1997: Earth's annual global mean energy budget. *Bull. Amer. Meteor. Soc.*, **78**, 197–208.

McFarquhar, G. M., and A. J. Heymsfield, 1997: Parameterization of tropical cirrus ice crystal size distributions and implications for radiative transfer: Results from CEPEX. *J. Atmos. Sci.*, **54**, 2187–2200.

Pincus, R., and M. Baker, 1994: Effect of precipitation on the albedo susceptibility of clouds in the marine boundary layer. *Nature*, **372**, 250–252.

Siebesma, A. P., and Coauthors, 2003: A large eddy simulation intercomparison study of shallow cumulus convection. *J. Atmos. Sci.*, **60**, 1201–1219.

Smolarkiewicz, P. K., and L. G. Margolin, 1997: On forward-in-time differencing for fluids: An Eulerian/semi-Lagrangian nonhydrostatic model for stratified flows. *Atmos.-Ocean Special*, **35**, 127–152.

Stephens, G. L., 1978: Radiation profiles in extended water clouds. II: Parameterization schemes. *J. Atmos. Sci.*, **35**, 2123–2132.

Troen, I., and L. Mahrt, 1986: A simple model of the atmospheric boundary layer; sensitivity to surface evaporation. *Bound.-Layer Meteor.*, **37**, 129–148.

Twomey, S., 1974: Pollution and the planetary albedo. *Atmos. Envir.*, **8**, 1251–1256.

Twomey, S., 1977: The influence of pollution on the shortwave albedo of clouds. *J. Atmos. Sci.*, **34**, 1149–1152.

Warner, J., 1968: A reduction of rainfall associated with smoke from sugar-cane fires - An inadvertent weather modification. *J. Appl. Meteorol.*, **7**, 247–251.